Journal of Microbiology (2022) Vol. 60, No. 7, pp. 705–714
DOI 10.1007/s12275-022-2204-y
eISSN 1976-3794
pISSN 1225-8873

Yeast polyubiquitin unit regulates synaptonemal complex formation and recombination during meiosis[§]

Min-Kyung Jo, Kiwon Rhee, Keun Pil Kim*, and Soogil Hong*

Department of Life Sciences, Chung-Ang University, Seoul 06974, Republic of Korea

(Received May 9, 2022 / Revised Jun 9, 2022 / Accepted Jun 10, 2022)

Ubiquitin is highly conserved in most eukaryotes and involved in diverse physiological processes, including cell division, protein quality control, and protein degradation mediated by the ubiquitin-proteasome system after heat shock, glucose-starvation, and oxidative stress. However, the role of the ubiquitin gene *UBI4*, which contains five consecutive head-to-tail ubiquitin repeats, in meiosis has not been investigated. In this study, we show that the *Saccharomyces cerevisiae* polyubiquitin precursor gene, *UBI4*, is required to promote synaptonemal complex (SC) formation and suppress excess double-strand break formation. Moreover, the proportion of Zip1 polycomplexes, which indicate abnormal SC formation, in cells with a mutation in *UBI4* (i.e., *ubi4Δ* cells) is higher than that of wild-type cells, implying that the *UBI4* plays an important role in the early meiotic prophase I. Interestingly, although *ubi4Δ* cells rarely form full-length SCs in the pachytene stage of prophase I, the Zip3 foci are still seen, as in wild-type cells. Moreover, *ubi4Δ* cells proficiently form crossover and noncrossover products with a slight delay compared to wild-type cells, suggesting that *UBI4* is dispensable in SC-coupled recombination. Our findings demonstrate that *UBI4* exhibits dual functions that are associated with both positive and negative roles in SC formation and recombination during meiosis.

Keywords: ubiquitin, *UBI4*, meiosis, recombination

Introduction

Meiosis is a specialized cell cycle that generates haploid progenitor cells after two rounds of cell division (Petronczki *et al.*, 2003; Hunter, 2015). During meiosis, genetic recombination occurs between the parental chromosomes in prophase I and generally promotes faithful chromosome segregation (Zickler and Kleckner, 2015). Meiotic chromosomes appear to favor the exchange of genes between homologs over sister chromatids (Hunter, 2006). In this process, homologous chromosomes are paired together by the synaptonemal complex (SC), which creates a meiosis-specific chromosome linkage along the entire length of chromosomes (Kleckner, 2006; Zickler and Kleckner, 2015). The SC contains a central region with polymerized transverse filaments flanked by two homologous chromosomal axes with multiple chromatin loops (Cahoon and Hawley, 2016; Gao and Colaiacovo, 2018). In meiotic prophase I, homologous chromosomes align across the entire length of the chromosome (Zickler and Kleckner, 1999; Gray and Cohen, 2016). The elongation of SCs occurs in the pachytene stage of prophase I and forms full-length SCs (Zickler and Kleckner, 1999; Page and Hawley, 2004; Hong *et al.*, 2019a). Synapses on homologous chromosomes, which lead to SC formation, begin at specific sites along the chromosome corresponding to the site of meiotic recombination. Zip, Msh, Mer (ZMM), and synapsis initiation complex (SIC), including Zip1-4, Msh4/5, Mer3, Spo16, Pph3, and EG complex, promote SC formation and crossover (CO) recombination (Sym *et al.*, 1993; Sym and Roeder, 1995; Chua and Roeder, 1998; Agarwal and Roeder, 2000; Dong and Roeder, 2000; Börner *et al.*, 2004; Fung *et al.*, 2004; Lynn *et al.*, 2007; Shinohara *et al.*, 2008; Humphryes *et al.*, 2013; Voelkel-Meiman *et al.*, 2013; Leung *et al.*, 2015; Lee *et al.*, 2021). CO-designated recombination intermediates mature mostly within the SC structure, and SCs positively correlate with CO formation (Börner *et al.*, 2004; Shinohara *et al.*, 2008). Previous studies have demonstrated that although SC formation is important for CO formation, defects in SC structure increase CO levels (Libuda *et al.*, 2013; Wang *et al.*, 2015; Voelkel-Meiman *et al.*, 2016; Lee *et al.*, 2021).

The ubiquitin-proteasome system (UPS) is required for many cellular processes; it highly regulates protein degradation, protein quality control, and the cell cycle (Hochstrasser, 1996; Ciechanover and Schwartz, 1998; Finley, 2009). In the UPS, ubiquitin is covalently bound via its C-terminus Glycine residue to a substrate protein, a process called "polyubiquitination" (Schlesinger and Goldstein, 1975; Dworkin-Rastl *et al.*, 1984; Özkaynak *et al.*, 1984; Bond and Schlesinger, 1985; Wiborg *et al.*, 1985). Furthermore, ubiquitin is essential for survival in many stress environments, such as oxidative stress and heat shock, that cause protein misfolding and aggregation (Goldberg, 2003; Amm *et al.*, 2013; Shiber *et al.*, 2013). Therefore, the expression of stress-response genes and active ubiquitination are parts of the heat shock response, which allows cells to survive (Parag *et al.*, 1987; Fang *et al.*, 2011, 2014). Recent genetic and microscopic data from budding yeast have shown that budding yeast SCF^{cdc4} ubiquitin ligase regulates SC formation and plays distinct roles in SC forma-

*For correspondence. (S. Hong) E-mail: hsg-richer@daum.net / (K.P. Kim) E-mail: kpkim@cau.ac.kr
[§]Supplemental material for this article may be found at https://doi.org/10.1007/s12275-022-2204-y.

tion and recombination independent of Zip3 (Zhu *et al.*, 2020). Interestingly, full SC assembly is not required for recombination under depletion conditions of CDC53, a cullin protein of SCF ubiquitin ligase (Zhu *et al.*, 2020; Yang *et al.*, 2022). Pre9, a yeast α3 proteasome subunit, is required for double-strand break (DSB) formation, chromosome morphogenesis, and CO-designated recombination (Ahuja *et al.*, 2017). Furthermore, *Hei10*$^{mei4/mei4}$ spermatocytes exhibit delayed meiotic DSB repair and defective CO formation (Qiao *et al.*, 2014). Thus, these observations indicate that UPSs are directly or indirectly associated with chromosomal organization and recombination during meiosis.

In the yeast *Saccharomyces cerevisiae*, three different genes, *UBI1*, *UBI2*, and *UBI3*, encode monomeric ubiquitin (Wiborg *et al.*, 1985; Özkaynak *et al.*, 1987). Additionally, *UBI4* specifically encodes a polyubiquitin precursor protein containing five ubiquitin repeats that are subsequently cleaved by deubiquitinating enzymes to release monomeric ubiquitin (Özkaynak *et al.*, 1984; Finley *et al.*, 1987; Gemayel *et al.*, 2017). The expression of *UBI4* increases during high-temperature exposure, glucose starvation, oxidative stress, and sporulation (meiosis) (Bachmair *et al.*, 1986; Finley *et al.*, 1987; Tanaka *et al.*, 1988; Treger *et al.*, 1988; Watt and Piper, 1997; Okazaki *et al.*, 2000; Cheng *et al.*, 2006; Bhagwat *et al.*, 2021), suggesting that the expression of *UBI4* is involved in the survival of various stressors through the ubiquitin-mediated proteasome pathway (Okazaki *et al.*, 2000). Yeast *UBI4* plays an important role in heat shock, oxidative stresses, and zinc deficiency (Cheng *et al.*, 1994; Simon *et al.*, 1999; MacDiarmid *et al.*, 2016). The expression of *UBI4* increases after heat stress upon exposure to DNA damage chemicals, and the number of ubiquitin units encoded by *UBI4* influences the cell survival rate (Gemayel *et al.*, 2017). In the *Saccharomyces* genus, the number of repeats in *UBI4* directly influences the UPS and cell viability under stress conditions (Gemayel *et al.*, 2017). However, the detailed functional role of the polyubiquitin gene *UBI4* in chromosome organization and recombination during meiosis remains unknown.

In the present study, we describe the roles of *UBI4* in yeast for chromosome organization, programmed DSB formation, and genetic recombination, specifically occurring in prophase I of meiosis. We found that *UBI4* is required to promote chromosome axis/SC formation and that SC assembly is uncoupled from CO recombination in *ubi4Δ* cells. Moreover, *UBI4* suppresses additional DSB formation in early prophase I at the *HIS4LEU2* locus. Thus, our findings demonstrate that *UBI4* is essential for forming chromosomal SC structures as well as for homeostatic control of DSB formation in meiosis.

Materials and Methods

Strains

All yeast strains in this study were derivatives of *S. cerevisiae* SK1 strains. Detailed information on the genotypes and strains is provided in Supplementary data Table S1.

DNA-damaging agent sensitivity test

The cells were grown to saturation in YPD media (1% yeast extract, 2% peptone, and 2% glucose) at 30°C for 1 day. Their optical density (OD) values were calculated, adjusted to 0.6 at 600 nm. The solutions of saturated cells were then serially diluted 10-fold in YPD media (10^{-1}, 10^{-2}, 10^{-3}, 10^{-4}, and 10^{-5}) and spotted onto YPD plates (1% yeast extract, 2% peptone, 2% agar, and 2% glucose) containing DNA-damaging agents: methyl methanesulfonate (MMS; 0.015%), camptothecin (CPT; 1 μg/ml), and hydroxyurea (HU; 40 mM). Plates were incubated for 3 days at 30°C or 37°C and evaluated for cell growth.

Meiotic time course

The time-course experiment was performed as previously described (Kim *et al.*, 2010; Hong *et al.*, 2013, 2019b; Cho *et al.*, 2016; Yoon *et al.*, 2016; Kong *et al.*, 2017; Lee *et al.*, 2021; Joo *et al.*, 2022). Yeast cells were patched onto a YPG plate (1% yeast extract, 2% peptone, 2% agar, and 3% glycerol) and incubated at 30°C for 18 h. The cells were then streaked onto a YPD plate and incubated at 30°C for 2 days. A single colony was picked, inoculated into 2 ml of YPD liquid medium (1% yeast extract, 2% peptone, and 2% glucose), and placed in a shaking incubator at 30°C for 1 day. The saturated-at-stationary phase yeast cells were diluted in 200 ml of pre-warmed SPS medium (SPS; 0.5% yeast extract, 1% peptone, 0.17% yeast nitrogen base without amino acids, 0.5% ammonium sulfate, 1% potassium acetate, and 50 mM potassium biphthalate; pH was adjusted to 5.5 with 10 M KOH) and placed in a shaking incubator for 18 h at 30°C. Cells synchronized in the G1 phase were resuspended in a pre-warmed sporulation medium (SPM; 1% potassium acetate, 0.02% raffinose, and 2 drops/L antifoam) to induce meiosis. To investigate meiotic division and recombination, we harvested the yeast cells at different time points (0, 2.5, 3.5, 4, 5, 6, 7, 8, 10, and 24 h) and cross-linked them in 0.1 mg/ml trioxsalen (Sigma, T1637) by exposure to 365-nm UV light for 15 min. We fixed a portion of cells with 40% ethanol and 0.1 M sorbitol to allow us to monitor meiotic nuclear division. Nuclei were stained with 1 μg/ml 4′,6-diamidino-2-phenylindole (DAPI), and about 200 nuclei were observed using fluorescence microscopy (Olympus BX53).

Chromosome spreading and immunofluorescence

Yeast meiotic chromosome spreads for immunofluorescence microscopy were performed as previously described (Kim *et al.*, 2010; Yoon *et al.*, 2016; Hong *et al.*, 2019b; Joo *et al.*, 2022). Yeast cells were lysed with 1% Lipsol and fixed with 3% paraformaldehyde and 3.4% sucrose buffer. The slides were soaked in 0.2% Photo-Flo 200 (Kodak, 146–4510) for 30 sec and then washed with 1X TBS buffer (136 mM NaCl, 3 mM KCl, and 25 mM Tris-HCl; pH 7.5) for 15 min. The following antibodies were used in this study: rabbit polyclonal Zip1 antibody (primary; diluted 1:500, Custom); mouse monoclonal Myc antibody (primary; diluted 1:500; Santa Cruz Biotechnology, sc-40); mouse polyclonal HA antibody (primary; diluted 1:500; Santa Cruz Biotechnology, sc-7392); TRITC-conjugated goat anti-rabbit lgG secondary antibody (diluted 1:300; Jackson ImmunoResearch, 111–025-003); Alexa 488-

conjugated goat anti-mouse IgG secondary antibody (diluted 1:300; Jackson ImmunoResearch, 115–545-003). All images were acquired using a Nikon Eclipse Ti fluorescence microscope equipped with a Nikon DS-Qi2 monochrome camera, and deconvolution was adjusted with Nikon NIS software (Nikon).

Genomic DNA extraction

Genomic DNA was extracted as previously described (Kim *et al*., 2010; Hong *et al*., 2013, 2019b; Cho *et al*., 2016; Yoon *et al*., 2016; Kong *et al*., 2017; Lee *et al*., 2021; Joo *et al*., 2022). The cells were incubated in a guanidine-HCl solution (4.5 M Guanidine-HCl, 0.1 M EDTA, 0.15 M NaCl, and 0.05% sodium lauroyl sarcosinate) at 65°C for 15 min. The lysed cells were treated with RNase solution (100 mM Tris-HCl, 10 mM EDTA, and 50 mg/ml RNase A; Sigma, R6513) at 37°C for 60 min. Proteinase K (Enzynomics, PR003) was added to each sample, and the samples were incubated at 65°C for 60 min. Phenol/chloroform/isoamyl alcohol (Biosolution, BP026) was added to the genomic DNA samples and precipitated with ethanol and 3 M sodium acetate. DNA pellets were completely dissolved in TE buffer (50 mM Tris-HCl and 1 mM EDTA).

Southern hybridization

The physical analysis of recombination at the *HIS4LUE2* locus was performed as described previously (Kim *et al*., 2010; Hong *et al*., 2013, 2019b; Cho *et al*., 2016; Yoon *et al*., 2016; Kong *et al*., 2017; Lee *et al*., 2021; Joo *et al*., 2022). The extracted yeast genomic DNA (2 μg) was digested with restriction enzymes (*Xho*I or *Xho*I and *NgoM*IV) for one-dimensional (1D) gel analysis. For two-dimensional (2D) gel analysis, the extracted yeast genomic DNA (2.5 μg) was digested with *Xho*I. The digested genomic DNA samples for 1D gel analysis were loaded onto agarose gels (0.6% UltraKem LE agarose (Young Science, Y50004) in 1X TBE buffer) and electrophoresed in 1X TBE buffer for 24 h. The DNA samples for 2D gel analysis were loaded onto agarose gels (0.4% Seakem Gold agarose [Lonza, 50152] in 1X TBE buffer) and electrophoresed in 1X TBE buffer for 21 h. The agarose gels were stained with 0.5 μg/mL ethidium bromide (EtBr). For 2D gel analysis, the strips of interest were sliced and placed in a 2D tray. Agarose gel (0.8% UltraKem LE agarose containing EtBr in 1X TBE buffer) was poured and allowed to solidify. The gel was then electrophoresed in 1X TBE buffer for 6 h at 4°C. Southern blotting was performed. Briefly, the gel was soaked in 0.25 N HCl for 20 min, washed with distilled water, and then soaked in 0.4 M NaOH for 30 min. The DNA species on the gel were transferred to a Biodyne B membrane (Pall, PA60208). Hybridization was performed using specific probe A ^{32}P-dCTP-labeled nucleotides and a random priming DNA labeling kit (Agilent Technologies, 300392). Hybridization DNA species signals were visualized using a phospho-image analyzer (Bio-Rad). These signals were quantified with the Quantity One software (Bio-Rad).

Results

UBI4 influences DNA damage repair at high temperatures

In *S. cerevisiae* SK1 strains, *UBI4* is translated into a five-ubiquitin protein that is subsequently processed by a deubiquitination enzyme to produce monomeric ubiquitin (Fig. 1A). However, the function and modulatory role of *UBI4* in DNA damage and meiosis remains unknown. To delineate

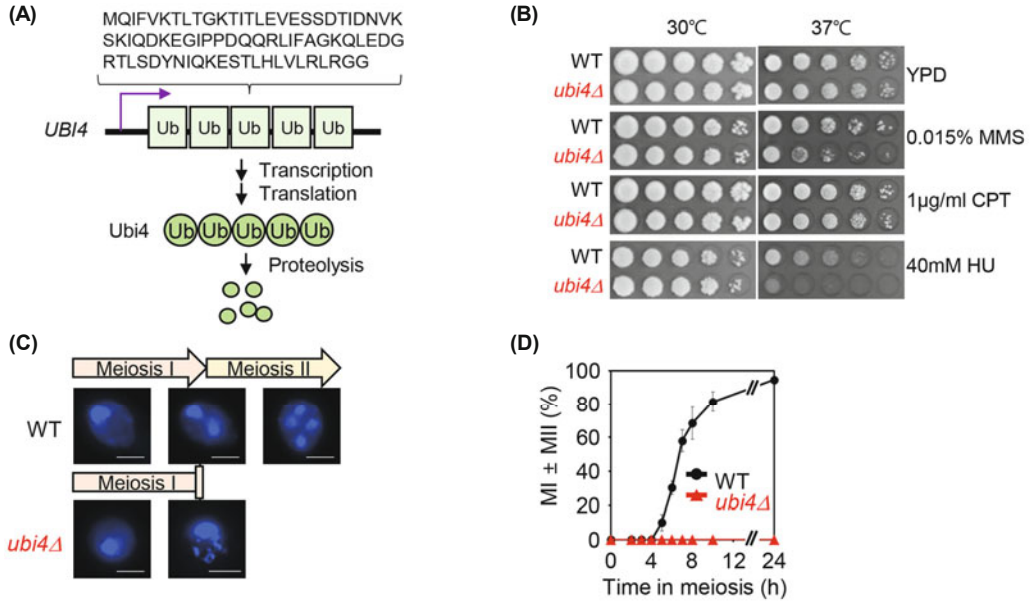

Fig. 1. DNA-damaging agent sensitivity and meiotic division in WT and *ubi4Δ* cells. (A) Illustration of *UBI4* gene that encodes five repeats of ubiquitin. The polyubiquitin unit is degraded by proteolysis after translation. (B) DNA-damaging agent sensitivity test. Yeast cells were cultured at 30°C and 37°C with or without DNA-damaging chemicals in WT and *ubi4Δ* cells. (C) Meiotic nuclei in WT and *ubi4Δ* cells. Representative images of nuclei stained with DAPI (meiosis I, MI; meiosis II, MII). The scale bars indicate 2.5 μm. (D) Meiotic division in WT and *ubi4Δ* cells (> 200 cells were counted).

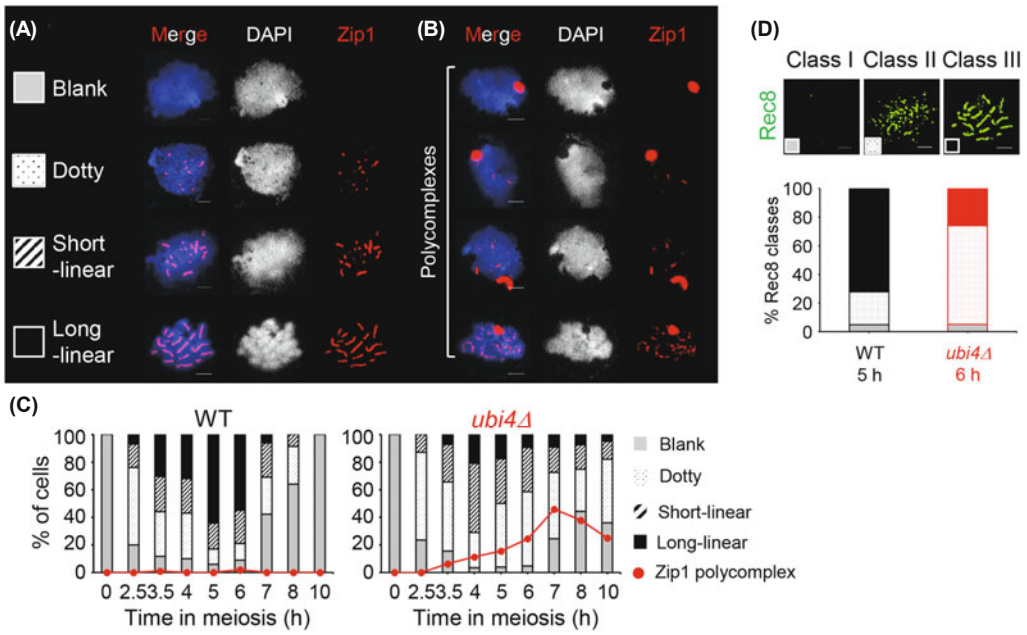

Fig. 2. Chromosome axis and synaptonemal complex formation in WT and *ubi4Δ* cells. (A) Representative images of chromosome spreads of meiotic cells immunostained for Zip1 protein. Blank, no Zip1 staining; dotty, punctate Zip1 staining; short-linear, short Zip1-stained lines; long-linear, completely stained Zip1 lines. Scale bar: 2.5 μm. (B) Representative images of polycomplexes (PCs) during the prophase I. Scale bar: 2.5 μm. (C) Quantification of Zip1 staining types in WT and *ubi4Δ* cells. The immunostained nuclei were classified according to the shape of the Zip1 staining. The red line indicates the percentage of polycomplexes. More than 100 nuclei were counted at each time point. (D) Representative images of chromosome spreads of meiotic cells immunostained for Rec8. Blank, no Rec8 staining; short, punctate Rec8 staining; long-linear, completely stained Rec8 lines. The scale bars indicate 2.5 μm (upper panel). Quantification of Rec8 staining types at the pachytene stage in WT and *ubi4Δ* cells.

the role of *UBI4* in DNA damage repair, an SK1 strain carrying the *ubi4Δ* mutation was examined for sensitivity to genotoxic agents including MMS, CPT, and HU. Both WT and *ubi4Δ* cells were not sensitive to the genotoxic agents and exhibited no defects in growth at 30°C. In contrast, *ubi4Δ* was sensitive to the reagents at 37°C (Fig. 1B), indicating that *UBI4* is essential to DNA repair under high-temperature conditions.

Absence of *UBI4* induces meiotic prophase arrest

UBI4 transcripts accumulate during sporulation (i.e., meiosis) of *S. cerevisiae* and function during starvation and heat stress (Finley *et al.*, 1987; Tanaka *et al.*, 1988). To investigate the role of *UBI4* in meiosis, we analyzed the timing of replication, nuclear division, and sporulation using DAPI staining. Although the *ubi4Δ* cells grew normally during mitosis at 30°C, pre-meiotic DNA replication was delayed by approximately 0.5 h compared to WT cells (Fig. 1C; Supplementary data Fig. S1). In WT cells, nuclei staining showed that meiosis I begins approximately 6 h after synchronized cells are transferred to SPM; about 58% of cells had completed MI or MI/MII divisions at 7 h. In contrast, *ubi4Δ* cells were arrested before the onset of meiosis I: dyads or tetrads were undetectable until 24 h (Fig. 1D). Thus, *ubi4Δ* cells fail to segregate their chromosomes and are defective in meiosis. These results are consistent with previous findings demonstrating that *ubi4Δ* mutants are viable as vegetative cells but sporulation-defective (Finley *et al.*, 1987).

ubi4Δ mutant exhibits defective chromosome axis and SC formation

ZMM proteins are involved in class I CO recombination and SC formation during meiosis (Zickler and Kleckner, 1999; Allers and Lichten, 2001; Börner *et al.*, 2004; Kleckner, 2006; Lynn *et al.*, 2007; Shinohara *et al.*, 2008). Thus, CO-fate recombination is associated with SC formation. However, some mutants exhibit an increase in CO formation with elevated DSB levels even if SC formation is defective (Libuda *et al.*, 2013; Wang *et al.*, 2015; Voelkel-Meiman *et al.*, 2016; Lee *et al.*, 2021). Further, although Cdc53 depletion in the Skp-Cullin-F-box ubiquitin ligase leads to normal levels of meiotic recombination, chromosome axis/SC formation is defective in such cells (Zhu *et al.*, 2020). To determine the effect of *UBI4* on SC formation, we examined the assembly of Zip1 that promotes SC formation and CO-fate recombination in prophase I. Chromosome spreads were classified into four categories dependent on Zip1 staining signals: Class I (no Zip1 signals), Class II (Zip1 foci), Class III (Zip1 foci and short-linear), and Class IV (Zip1 long-linear) (Fig. 2A). In WT cells, short Zip1 staining was observed in early prophase I. In the mid/late-pachytene stage, when SCs form along the entire length, Zip1 exhibits long-lined staining patterns (Fig. 2C). The *ubi4Δ* cells had fewer full SC formations (Class IV) and an apparently elevated proportion of Zip1 polycomplexes, which indicates an abnormal aggregation of Zip1 proteins, implying a defect in installing SC along the chromosomes during the zygotene/pachytene stages (Fig. 2B and C).

Thus, our Zip1 assembly experiments suggest defective SC formation in *ubi4Δ* cells.

We were therefore interested in examining whether *ubi4Δ* cells exhibit typical chromosome axis formation. Rec8 associates with the cohesin complex and is a prominent chromosome axis protein in meiotic prophase I (Molnar *et al*., 1995; Klein *et al*., 1999). The chromosome axis is integrated into the SC when homologous chromosomes physically interact and pair during the zygotene stage of prophase I. Zip1-mediated SC formation could therefore be dependent on Rec8-mediated cohesin complex formation. We characterized chromosome axis morphogenesis using Rec8 staining in *ubi4Δ* cells relative to WT cells. Surface-spread nuclei were assessed for Rec8 staining signals and classified into three previously defined classes (Yoon *et al*., 2016): Class I, no Rec8 staining signals; Class II, a large number of foci with short lines (leptotene/zygotene); and Class III, long staining lines (zygotene/pachytene). In WT cells, 73% of Rec8-positive nuclei exhibit full-length Rec8 staining (Class III) in prophase I (Fig. 2D). However, the *ubi4Δ* cells exhibited a Class II staining pattern, implying normal progression of axis formation, but defective full-length Rec8 staining (26%), consistent with the aberrant assemblies of Zip1 (Fig. 2D). The *ubi4Δ* cells progressed to Class II at high levels and exhibited a significant defect in Class III Rec8 staining compared to WT, implying a severe defect in normal SC formation during the zygotene/pachytene stages.

ubi4Δ cells exhibit normal Zip3 focus formation

Zip3 prominently localizes to the sites of CO-designated recombination interaction (Agarwal and Roeder, 2000; Fung *et al*., 2004; Cheng *et al*., 2006; Zhang *et al*., 2014), and stabilizes the transition of D-loop to SEI, which is clearly detected during the mid-pachytene stage of prophase I (Agarwal and Roeder, 2000; Yoon *et al*., 2016; Hong *et al*., 2019a; Lee *et al*., 2021). Here, we investigated Zip3 focus formation in WT and *ubi4Δ* cells using a Myc tag inserted at the C-terminus of Zip3 protein (Fig. 3A and B). In WT cells, we observed an average of 46.3 and 54.32 Zip3 foci at 4 h and 5 h, respectively (Fig. 3C), which became progressively undetectable (data not shown). By comparison, we detected an average of 50.5 and 49.5 Zip3 foci in *ubi4Δ* cells at 5 h and 6 h, respectively, levels that are similar to those found in WT cells (Fig. 3C). These data indicate that Zip3 loading is normal for CO-fate recombination in *ubi4Δ* cells that show aberrant SC formation.

ubi4Δ cells exhibit increased DSB formation

In budding yeast, recombination frequencies are lower in mutant strains that are missing proteins required for chromosome axis/SC formation, such as *rec8Δ*, *zip1Δ*, *zip2Δ*, *zip4Δ*, and *msh4Δ* (Börner *et al*., 2004; Tsubouchi *et al*., 2006; Kim *et al*., 2010; Pyatnitskaya *et al*., 2019; He *et al*., 2020; Nandanan *et al*., 2021). To investigate meiotic recombination in *ubi4Δ* cells, we used a physical assay system (i.e., Southern blotting) to analyze meiotic DSB formation at the *HIS4LEU2* locus, which contains a single DSB hot spot (Fig. 4A). DNA events of recombination were monitored over time in SPM cultures. In WT cells, DSBs appear at 2.5 h after transfer to

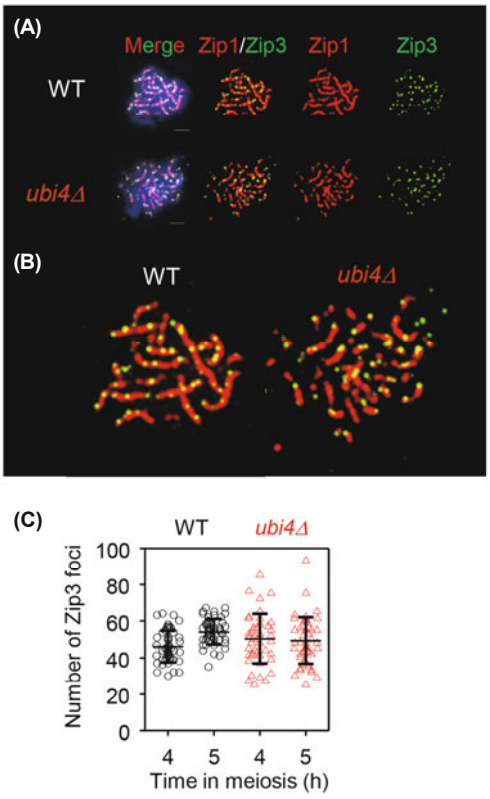

Fig. 3. Zip3 focus formation in WT and *ubi4Δ* cells. (A) and (B) Representative images of chromosome spreads of meiotic cells at the pachytene stage in WT and *ubi4Δ* cells. Red, Zip1; green, Zip3. The scale bars indicate 2.5 μm. (C) Zip3 foci per nucleus in WT and *ubi4Δ* cells. The error bars are the mean ± SD from three independent biological replicates.

SPM and peak at 3.5 h with 6.28 ± 0.45% of total hybridizing DNA signals (Fig. 4B and C). DSB initiation timing is similar in *ubi4Δ* cells, and the maximum levels observed in *ubi4Δ* cells are similar to those in WT cells. However, in a *rad50S* background where DSBs accumulate rather than progress to recombination intermediates, the *ubi4Δ* cells had a higher DSB level by 29 ± 1.62% compared to *rad50S* (24 ± 2.90%) at the *HIS4LEU2* locus (Fig. 4D and E; Supplementary data Fig. S2). The excess DSBs when *UBI4* is absent in meiosis suggest that *UBI4* suppresses DSB formation in early prophase I.

ubi4Δ cells exhibit increased numbers of CO and NCO

We next used the physical analysis of recombination to explore how the excess DSBs in *ubi4Δ* cells progress to CO or noncrossover (NCO) products. In WT cells, COs began to form at 4 h and reached a maximum level at 24 h (15.3 ± 1.28%), and the total levels of CO and NCO species were 3.79 ± 1.17% and 3.19 ± 0.91%, respectively, with maximum levels at 24 h (Fig. 4F and G). By comparison, the *ubi4Δ* mutant cells formed more CO (5.86 ± 0.83%) and NCO (5.97 ± 0.77%), with a delay in the time to reach maximum levels; however, NCO levels were modestly higher than CO levels (Fig. 4F and G). These results suggest that the *ubi4Δ* mutant cells may have formed more COs and NCOs since they contain more DSBs than WT cells (Supplementary data Fig. S2).

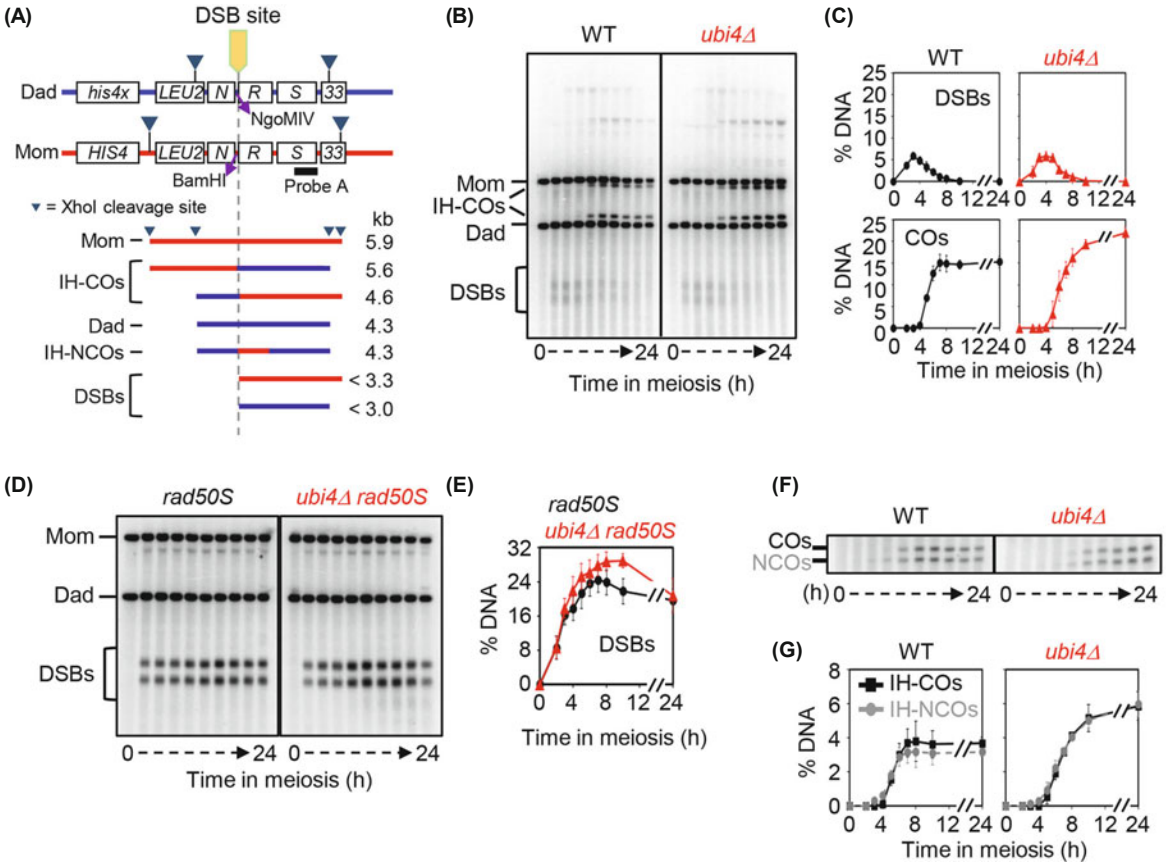

Fig. 4. 1D gel of DNA physical assay of meiotic recombination in WT and *ubi4Δ* cells. (A) Map of the *HIS4LUE2* hot spot located on chromosome III. "Mom" and "Dad" chromosomes have *Xho*I restriction enzyme sites. Specific probe A visualizes a variety of DNA species. Mom, mom species; Dad, dad species; COs, crossovers; NCOs, noncrossovers; DSBs, double-strand breaks. (B) Representative image of 1D gel from WT and *ubi4Δ* cells. (C) Quantitative analysis of the DSBs and COs in (B). Black circle, WT; red triangle, *ubi4Δ*. (D) Representative image of 1D gel from *rad50S* and *ubi4Δ rad50S* cells. (E) Quantitative analysis of the DSBs in (F). Black circle, WT; red triangle, *ubi4Δ*. (F) Representative image of CO/NCO gel from WT and *ubi4Δ* cells. (G) Quantitative analysis of the COs and NCOs in (D). Black square, COs; gray circle, NCOs. Data are the mean ± SD (N = 3).

ubi4Δ cells exhibit delay in the CO pathway

To further investigate whether the extra DSBs progress to form joint molecules (JMs), we analyzed single end invasions (SEIs) and double Holliday junctions (dHJs) using native/native 2D gel electrophoresis followed by Southern blotting (Fig. 5A and B). This analysis can reveal the recombination intermediates, SEIs and dHJs identified previously, and the progression of recombination (Hunter and Kleckner, 2001; Kim *et al.*, 2010; Hong *et al.*, 2013; Lee *et al.*, 2021). In WT cells, SEIs and dHJs were detected after 3.5 h and reached a maximum level at 4 h. In the *ubi4Δ* cells, SEIs and dHJs were observed after 3.5 h, but reached a maximum level at 5 h, showing a delay in peak levels compared to WT cells (Fig. 5C and D; Supplementary data Fig. S3). Furthermore, the steady-state levels of the detected SEIs and dHJs were higher in the *ubi4Δ* than in the WT cells (Fig. 5D; SEI = 1.90 ± 0.28% and dHJ = 1.51 ± 0.38% for WT; SEI = 2.14 ± 0.28% and dHJ = 1.77 ± 0.44% for *ubi4Δ*). However, the majority of the SEI and dHJ signals had disappeared by 10 h, similar to what we observed in WT cells (Supplementary data Fig. S3). The *ubi4Δ* cells exhibited an interhomolog bias (an IH:IS dHJ ratio of approximately 5:1) similar to that seen in WT cells (Fig. 5C and D). These results suggest both normal JM formation and a normal interhomolog bias, but higher JM levels in *ubi4Δ* compared to WT cells.

Discussion

Ubiquitin is a highly conserved 76-residue protein that is covalently attached to a variety of target proteins in most eukaryotes (Ciechanover and Schwartz, 1998; Hershko and Ciechanover, 1998). Yeast ubiquitin is encoded by a family of *UBI* genes including *UBI1*, *UBI2*, *UBI3*, and *UBI4* (Özkaynak *et al.*, 1987; Finley *et al.*, 1989). Specifically, the budding yeast *UBI4* gene, which encodes a polyubiquitin precursor protein, is essential for vegetable growth and regulated in response to diverse stress conditions, including heat stress, nutrient starvation, and oxidative stress (Finley *et al.*, 1987; Treger *et al.*, 1988). Furthermore, *UBI4* transcripts are highly accumulated after exposure to DNA-damaging reagents and sporulation conditions (Treger *et al.*, 1988). In this study, our data demonstrate that *UBI4* is required for proper SC formation and involved in the regulation of DSB formation during meiosis.

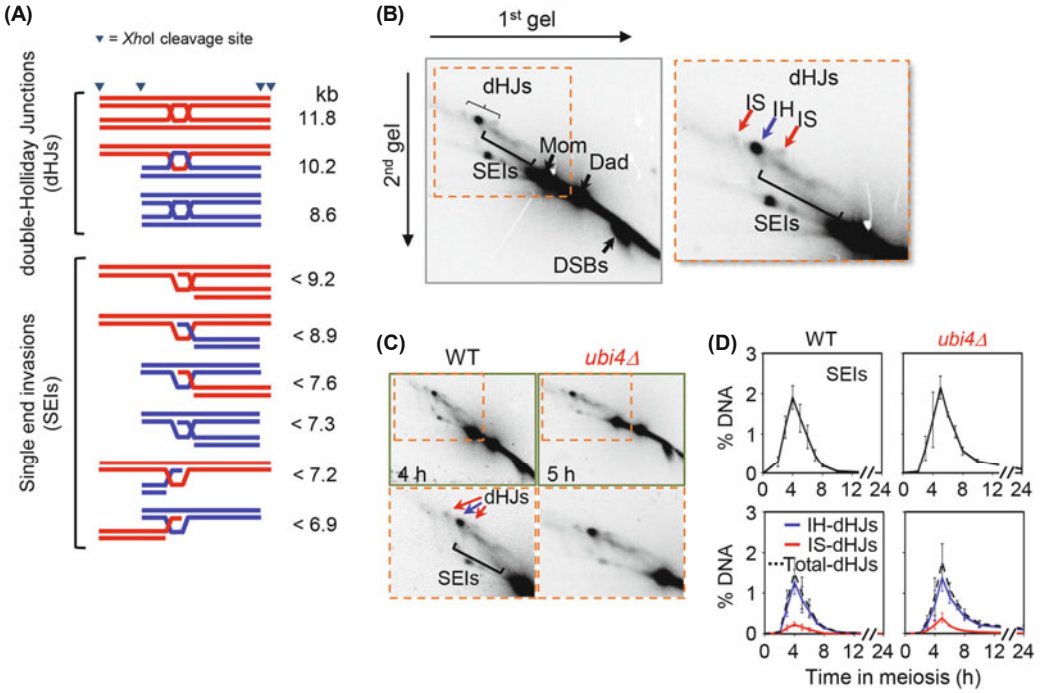

Fig. 5. 2D gel assay of meiotic recombination in WT and *ubi4Δ* cells. (A) Schematic diagram of JMs, dHJs, and SEIs. Mom (red) and Dad (blue). (B) Representative image of 2D gel from WT cells. Red arrow, IS-dHJs; blue arrow, IH-dHJs. (C) Representative images of 2D gel assay from WT (at 4 h) and *ubi4Δ* cells (at 5 h). (D) Quantification of SEIs (top) and dHJs (bottom) in WT and *ubi4Δ* cells. Data are the mean ± SD (N = 3).

UBI4 is dispensable for SC-associated recombination

During meiosis, several eukaryotes, including mice and yeast, express ubiquitin-mediated proteasome components, which are loaded on paired chromosomes and play a direct role in the chromosome axis and recombination pathway (Ahuja *et al*., 2017; Prasada Rao *et al*., 2017). Ubiquitin and proteasome are largely associated with chromosome axis and persist throughout pachynema of prophase I (Ahuja *et al*., 2017; Prasada Rao *et al*., 2017). In addition, mouse Hei10 ubiquitin ligase, which localizes to chromosome axis/SC and CO sites, is involved in CO and NCO differentiation (Qiao *et al*., 2014; Prasada Rao *et al*., 2017). Shinohara and colleagues have reported that SCF-dependent ubiquitination controls SC formation (Zhu *et al*., 2020). The absence of SCF ubiquitin ligase allows normal CO formation, but causes defective Zip1 assembly that is needed to form full SCs (Zhu *et al*., 2020), suggesting that SC formation might be negatively regulated in the absence of SCF ubiquitin ligase. Furthermore, in mouse meiosis, loading ubiquitin on the chromosome axis is essential for synapsis and CO recombination (Prasada Rao *et al*., 2017). We found the phenotype of *ubi4Δ* cells to be similar to that of *CDC53*-depleted cells: both exhibit defective SC formation but normal CO formation. Our results also show that the *ubi4Δ* mutation causes abnormal SC elongation and chromosome axis formation (Fig. 2), as seen in the absence of ubiquitin in mammalian meiosis. Meiotic DSBs, which occur in chromosome axis-associated recombination complexes, are dependent on the presence of Rec8 and axis proteins. Our classification of Zip1-Rec8 staining results indicates deficiencies in chromosome axis and SC formation in *ubi4Δ* cells. However, although *ubi4Δ* cells inefficiently form axes, they produce more DSBs than WT cells and form CO-designated JMs (Fig. 4).

Normal formation of CO and NCO despite aberrant SC formation

When CO- and NCO-designations have been established in the leptotene-to-zygotene transition, the CO recombination involves the formation of SEIs and dHJs in a ZMM-dependent manner called "Class I CO" (de los Santos *et al*., 2003; Page and Hawley, 2004; Lynn *et al*., 2007). A part of the DSBs can be repaired through a ZMM-independent pathway that yields both CO and NCO from the dHJ structures, called "Class II CO", which does not show interference (de los Santos *et al*., 2003; Page and Hawley, 2004; Lynn *et al*., 2007). Several lines of evidence suggest that Spo11-oligo levels and meiotic DSBs are increased in the defective synapsis, suggesting that SC formation negatively controls DSB formation (Kauppi *et al*., 2013; Thacker *et al*., 2014; Mu *et al*., 2020; Lee *et al*., 2021). In budding yeast, the *zmm* mutant exhibits higher DSB levels. However, CO-fated recombination is defective, but NCO recombination occurs at high levels in chromosome III. Two mutants with defective SC formation, *ecm11Δ* and *gmc2Δ*, have additional DSBs on a long chromosome VII during late prophase I. Our studies suggest that normal ZMM-dependent CO control may occur in the absence of *UBI4* and that DSB machineries continue to produce more DSB in early prophase I. In the *rad50S* background, both WT and *ubi4Δ* cells produced the same number of DSB until 4 h (early- or mid- pachytene stage), but *ubi4Δ* cells produced more DSB

later (mid- or late-pachytene) (Fig. 4E and F). This result further implies that SC formation might downregulate DSB formation. Moreover, our findings indicate that *ubi4Δ* cells exhibit defective SC formation and form extra DSBs on chromosome III that might produce more CO/NCO products (Fig. 4F and G). We therefore infer that *UBI4* is involved in the homeostatic control of meiotic DSB formation, and that this control might be influenced in a chromosome size-dependent manner. Thus, *UBI4*-dependent suppression of meiotic DSB formation may possibly occur through the degradation of proteins required for Spo11 activity. Previous studies have suggested that homeostatic regulation of DSB formation can be tightly regulated by ATM/ATR and homolog engagement (Zhang *et al*., 2011; Mohibullah and Keeney, 2017). In addition, proper loading of chromosome axis proteins, including Rec8, Red1, and Hop1, is required to form DSBs. Taken together, our findings suggest that Spo11 and/or axial proteins can persistently exist and therefore continue to promote DSB formation on meiotic chromosomes in *ubi4Δ* cells.

Acknowledgements

This research was supported by the National Research Foundation of Korea, funded by the Ministry of Science, ICT & Future Planning (2020R1A2C2011887) and by the Chung-Ang University Research Scholarship Grants in 2021.

Conflict of Interest

The authors have no conflict of interest to report.

References

Agarwal, S. and Roeder, G.S. 2000. Zip3 provides a link between recombination enzymes and synaptonemal complex proteins. *Cell* **102**, 245–255.

Ahuja, J.S., Sandhu, R., Mainpal, R., Lawson, C., Henley, H., Hunt, P.A., Yanowitz, J.L., and Börner, G.V. 2017. Control of meiotic pairing and recombination by chromosomally tethered 26*S* proteasome. *Science* **355**, 408–411.

Allers, T. and Lichten, M. 2001. Differential timing and control of noncrossover and crossover recombination during meiosis. *Cell* **106**, 47–57.

Amm, I., Sommer, T., and Wolf, D. 2013. Protein quality control and elimination of protein waste: the role of the ubiquitin-proteasome system. *Biochim. Biophys. Acta* **1843**, 182–196.

Bachmair, A., Finley, D., and Varshavsky, A. 1986. *In vivo* half-life of a protein is a function of its amino-terminal residue. *Science* **234**, 179–186.

Bhagwat, N.R., Owens, S.N., Ito, M., Boinapalli, J.V., Poa, P., Ditzel, A., Kopparapu, S., Mahalawat, M., Davies, O.R., Collins, S.R., *et al.* 2021. SUMO is a pervasive regulator of meiosis. *eLife* **10**, e57720.

Bond, U. and Schlesinger, M.J. 1985. Ubiquitin is a heat shock protein in chicken embryo fibroblasts. *Mol. Cell Biol.* **5**, 949–956.

Börner, G.V., Kleckner, N., and Hunter, N. 2004. Crossover/noncrossover differentiation, synaptonemal complex formation, and regulatory surveillance at the leptotene/zygotene transition of meiosis. *Cell* **117**, 29–45.

Cahoon, C.K. and Hawley R.S. 2016. Regulating the construction and demolition of the synaptonemal complex. *Nat. Struct. Mol. Biol.* **23**, 369–377.

Cheng, C.H., Lo, Y.H., Liang, S.S., Ti, S.C., Lin, F.M., Yeh, C.H., Huang, H.Y., and Wang, T.F. 2006. SUMO modifications control assembly of synaptonemal complex and polycomplex in meiosis of *Saccharomyces cerevisiae*. *Genes Dev.* **20**, 2067–2081.

Cheng, L., Watt, R., and Piper, P.W. 1994. Polyubiquitin gene expression contributes to oxidative stress resistance in respiratory yeast (*Saccharomyces cerevisiae*). *Mol. Gen. Genet.* **243**, 358–362.

Cho, H.R., Kong, Y.J., Hong, S.G., and Kim, K.P. 2016. Hop2 and Sae3 are required for Dmc1-mediated double-strand break repair via homolog bias during meiosis. *Mol. Cells* **39**, 550–556.

Chua, P.R. and Roeder, G.S. 1998. Zip2, a meiosis-specific protein required for the initiation of chromosome synapsis. *Cell* **93**, 349–359.

Ciechanover, A. and Schwartz, A.L. 1998. The ubiquitin-proteasome pathway: the complexity and myriad functions of proteins death. *Proc. Natl. Acad. Sci. USA* **95**, 2727–2730.

de los Santos, T., Hunter, N., Lee, C., Larkin, B., Loidl, J., and Hollingsworth, N.M. 2003. The Mus81/Mms4 endonuclease acts independently of double-Holliday junction resolution to promote a distinct subset of crossovers during meiosis in budding yeast. *Genetics* **164**, 81–94.

Dong, H. and Roeder, G.S. 2000. Organization of the yeast Zip1 protein within the central region of the synaptonemal complex. *J. Cell Biol.* **148**, 417–426.

Dworkin-Rastl, E., Shrutkowski, A., and Dworkin, M.B. 1984. Multiple ubiquitin mRNAs during xenopus laevis development contain tandem repeats of the 76 amino acid coding sequence. *Cell* **39**, 321–325.

Fang, N.N., Chan, G.T., Zhu, M., Comyn, S.A., Persaud, A., Deshaies, R.J., Rotin, D., Gsponer, J., and Mayor, T. 2014. Rsp5/Nedd4 is the main ubiquitin ligase that targets cytosolic misfolded proteins following heat stress. *Nat. Cell Biol.* **16**, 1227–1237.

Fang, N.N., Ng, A.H.M., Measday, V., and Mayor, T. 2011. Hul5 HECT ubiquitin ligase plays a major role in the ubiquitylation and turnover of cytosolic misfolded proteins. *Nat. Cell Biol.* **13**, 1344–1352.

Finley, D. 2009. Recognition and processing of ubiquitin-protein conjugates by the proteasome. *Annu. Rev. Biochem.* **78**, 477–513.

Finley, D., Bartel, B., and Varshavsky, A. 1989. The tails of ubiquitin precursors are ribosomal proteins whose fusion to ubiquitin facilitates ribosome biogenesis. *Nature* **338**, 394–401.

Finley, D., Ozkaynak, E., and Varshavsky, A. 1987. The yeast polyubiquitin gene is essential for resistance to high temperatures, starvation, and other stresses. *Cell* **48**, 1035–1046.

Fung, J.C., Rockmill, B., Odell, M., and Roeder, G.S. 2004. Imposition of crossover interference through the nonrandom distribution of synapsis initiation complexes. *Cell* **116**, 795–802.

Gao, J. and Colaiácovo, M.P. 2018. Zipping and unzipping: protein modifications regulating synaptonemal complex dynamics. *Trends Genet.* **34**, 232–245.

Gemayel, R., Yang, Y., Dzialo, M.C., Kominek, J., Vowinckel, J., Saels, V., Van Huffel, L., van der Zande, E., Ralser, M., Steensels, J., *et al.* 2017. Variable repeats in the eukaryotic polyubiquitin gene *ubi4* modulate proteostasis and stress survival. *Nat. Commun.* **8**, 397.

Goldberg, A.L. 2003. Protein degradation and protection against misfolded or damaged proteins. *Nature* **426**, 895–899.

Gray, S. and Cohen, P.E. 2016. Control of meiotic crossovers: from double-strand break formation of designation. *Annu. Rev. Genet.* **50**, 175–210.

He, W., Prasada Rao, H.B.D., Tang, S., Bhagwat, N., Kulkarni, D.S., Ma, Y., Chang, M., Hall, C., Bragg, J.W., Manasca, H.S., *et al.* 2020. Regulated proteolysis of MutSγ controls meiotic crossing over. *Mol. Cell* **78**, 168–183.

Hershko, A. and Ciechanover, A. 1998. The ubiquitin system. *Annu. Rev. Biochem.* **67**, 425–479.

Hochstrasser, M. 1996. Ubiquitin-dependent protein degradation. *Annu. Rev. Genet.* **30**, 405–439.

Hong, S., Joo, J.H., Yun, H., and Kim, K.P. 2019a. The nature of meiotic chromosome dynamics and recombination in budding yeast. *J. Microbiol.* **57**, 221–231.

Hong, S., Joo, J.H., Yun, H., Kleckner, N., and Kim, K.P. 2019b. Recruitment of Rec8, Pds5 and Rad61/Wapl to meiotic homolog pairing, recombination, axis formation and S-phase. *Nucleic Acids Res.* **47**, 11691–11708.

Hong, S., Sung, Y., Yu, M., Lee, M., Kleckner, N., and Kim, K.P. 2013. The logic and mechanism of homologous recombination partner choice. *Mol. Cell* **51**, 440–453.

Humphryes, N., Leung, W.K., Argunhan, B., Terentyev, Y., Dvorackova, M., and Tsubouchi, H. 2013. The Ecm11-Gmc2 complex promotes synaptonemal complex formation through assembly of transverse filaments in budding yeast. *PLoS Genet.* **9**, e1003194.

Hunter, N. 2006. Meiotic recombination. *In* Aguilera, A. and Rothstein, R. (eds.), Molecular Genetics of Recombination, vol. 17, pp. 381–442. Springer, Berlin, Heidelberg, Germany.

Hunter, N. 2015. Meiotic recombination: the essence of heredity. *Cold Spring Harb. Perspect. Biol.* **7**, a016618.

Hunter, N. and Kleckner, N. 2001. The single-end invasion: an asymmetric intermediate at the double-strand break to double-Holliday junction transition of meiotic recombination. *Cell* **106**, 59–70.

Joo, J.H., Kang, H.A., Kim, K.P., and Hong, S. 2022. Meiotic prophase roles of Pds5 in recombination and chromosome condensation in budding yeast. *J. Microbiol.* **60**,177–186.

Kauppi, L., Barchi, M., Lange, J., Baudat, F., Jasin, M., and Keeney, S. 2013. Numerical constraints and feedback control of double-strand breaks in mouse meiosis. *Genes Dev.* **27**, 873–886.

Kim, K.P., Weiner, B.M., Zhang, L., Jordan, A., Dekker, J., and Kleckner, N. 2010. Sister cohesion and structural axis components mediate homolog bias of meiotic recombination. *Cell* **143**, 924–937.

Kleckner, N. 2006. Chiasma formation: chromatin/axis interplay and the role(s) of the synaptonemal complex. *Chromosoma* **115**, 175–194.

Klein, F., Mahr, P., Galova, M., Buonomo, S.B., Michaelis, C., Nairz, K., and Nasmyth, K. 1999. A central role for cohesins in sister chromatid cohesion, formation of axial elements, and recombination during yeast meiosis. *Cell* **98**, 91–103.

Kong, Y.J., Joo, J.H., Kim, K.P., and Hong, S. 2017. Hed1 promotes meiotic crossover formation in *Saccharomyces cerevisiae*. *J. Microbiol. Biotechnol.* **27**, 405–411.

Lee, M.S., Higashide, M.T., Choi, H., Li, K., Hong, S., Lee, K., Shinohara, A., Shinohara, M., and Kim, K.P. 2021. The synaptonemal complex central region modulates crossover pathways and feedback control of meiotic double-strand break formation. *Nucleic Acids Res.* **49**, 7537–7553.

Leung, W.K., Humphryes, N., Afshar, N., Argunhan, B., Terentyev, Y., Tsubouchi, T., and Tsubouchi, H. 2015. The synaptonemal complex is assembled by a polySUMOylation-driven feedback mechanism in yeast. *J. Cell Biol.* **211**, 785–793.

Libuda, D.E., Uzawa, S., Meyer, B.J., and Villeneuve, A.M. 2013. Meiotic chromosome structures constrain and respond to designation of crossover sites. *Nature* **502**, 703–706.

Lynn, A., Soucek, R., and Börner, G.V. 2007. ZMM proteins during meiosis: crossover artists at work. *Chromosome Res.* **15**, 591–605.

MacDiarmid, C.W., Taggart, J., Jeong, J., Kerdsomboon, K., and Eide, D.J. 2016. Activation of the yeast *UBI4* polyubiquitin gene by Zap1 transcription factor via an intragenic promoter is critical for zinc-deficient growth. *J. Biol. Chem.* **291**, 18880–18896.

Mohibullah, N. and Keeney, S. 2017. Numerical and spatial patterning of yeast meiotic DNA breaks by Tel1. *Genome Res.* **27**, 278–288.

Molnar, M., Bähler, J., Sipiczki, M., and Kohli, J. 1995. The *rec8* gene of *Schizosaccharomyces pombe* is involved in linear element formation, chromosome pairing and sister-chromatid cohesion during meiosis. *Genetics* **141**, 61–73.

Mu, X., Murakami, H., Mohibullah, N., and Keeney, S. 2020. Chromosome-autonomous feedback down-regulates meiotic DNA break competence upon synaptonemal complex formation. *Genes Dev.* **34**, 1605–1618.

Nandanan, K.G., Salim, S., Pankajam, A.V., Shinohara, M., Lin, G., Chakraborty, P., Farnaz, A., Steinmetz, L.M., Shinohara, A., and Nishant, K.T. 2021. Regulation of Msh4-Msh5 association with meiotic chromosomes in budding yeast. *Genetics* **219**, iyab102.

Okazaki, K., Okayama, H., and Niwa, O. 2000. The polyubiquitin gene is essential for meiosis in fission yeast. *Exp. Cell Res.* **254**, 143–152.

Özkaynak, E., Finley, D., Solomon, M.J., and Varshavsky, A. 1987. The yeast ubiquitin genes: a family of natural gene fusions. *EMBO J.* **6**, 1429–1439.

Özkaynak, E., Finley, D., and Varshavsky, A. 1984. The yeast ubiquitin gene: head-to-tail repeats encoding a polyubiquitin precursor protein. *Nature* **312**, 663–666.

Page, S.L. and Hawley, R.S. 2004. The genetics and molecular biology of the synaptonemal complex. *Annu. Rev. Cell Dev. Biol.* **20**, 525–558.

Parag, H.A., Raboy, B., and Kulka, R.G. 1987. Effect of heat shock on protein degradation in mammalian cells: involvement of the ubiquitin system. *EMBO J.* **6**, 55–61.

Petronczki, M., Siomos., M.F., and Nasmyth, K. 2003. Un ménage à quatre: the molecular biology of chromosome segregation in meiosis. *Cell* **112**, 423–440.

Prasada Rao, H.B.D., Qiao, H., Bhatt, S.K., Bailey, L.R., Tran, H.D., Bourne, S.L., Qiu, W., Deshpande, A., Sharma, A.N., Beebout, C.J., *et al.* 2017. A SUMO-ubiquitin relay recruits proteasomes to chromosome axes to regulate meiotic recombination. *Science* **355**, 403–407.

Pyatnitskaya, A., Borde, V., and De Muyt, A. 2019. Crossing and zipping: molecular duties of the ZMM proteins in meiosis. *Chromosoma* **128**, 181–198.

Qiao, H., Prasada Rao, H.B.D., Yang, Y., Fong, J.H., Cloutier, J.M., Deacon, D.C., Nagel, K.E., Swartz, R.K., Strong, E., Holloway, J.K., *et al.* 2014. Antagonistic roles of ubiquitin ligase HEI10 and SUMO ligase RNF212 regulate meiotic recombination. *Nat. Genet.* **46**, 194–199.

Schlesinger, D.H. and Goldstein, G. 1975. Molecular conservation of 74 amino acid sequence of ubiquitin between cattle and man. *Nature* **255**, 423–424.

Shiber, A., Breuer, W., Brandeis, M., and Ravid, T. 2013. Ubiquitin conjugation triggers misfolded protein sequestration into quality control foci when Hsp70 chaperone levels are limiting. *Mol. Biol. Cell* **24**, 2076–2087.

Shinohara, M., Oh, S.D., Hunter, N., and Shinohara, A. 2008. Crossover assurance and crossover interference are distinctly regulated by the ZMM proteins during yeast meiosis. *Nat. Genet.* **40**, 299–309.

Simon, J.R., Treger, J.M., and McEntee, K. 1999. Multiple independent regulatory pathways control *UBI4* expression after heat shock in *Saccharomyces cerevisiae*. *Mol. Microbiol.* **31**, 823–832.

Sym, M., Engebrecht, J.A., and Roeder, G.S. 1993. ZIP1 is a synaptonemal complex protein required for meiotic chromosome synapsis. *Cell* **72**, 365–378.

Sym, M. and Roeder, G.S. 1995. Zip1-induced changes in synaptonemal complex structure and polycomplex assembly. *J. Cell Biol.* **128**, 455–466.

Tanaka, K., Matsumoto, K., and Toh-e, A. 1988. Dual regulation of the expression of the polyubiquitin gene by cyclic AMP and heat shock in yeast. *EMBO J.* **7**, 495–502.

Thacker, D., Mohibullah, N., Zhu, X., and Keeney, S. 2014. Homologue engagement controls meiotic DNA break number and distribution. *Nature* **510**, 241–246.

Treger, J.M., Heichman, K.A., and McEntee, K. 1988. Expression of the yeast *UBI4* gene increases in response to DNA damaging

agents and in meiosis. *Mol. Cell Biol.* **8**, 1132–1136.
Tsubouchi, T., Zhao, H., and Roeder, G.S. 2006. The meiosis-specific Zip4 protein regulates crossover distribution by promoting synaptonemal complex formation together with Zip2. *Dev. Cell* **10**, 809–819.
Voelkel-Meiman, K., Cheng, S.Y., Morehouse, S.J., and MacQueen, A.J. 2016. Synaptonemal complex proteins of budding yeast define reciprocal roles in MutSγ-mediated crossover formation. *Genetics* **203**, 1091–1103.
Voelkel-Meiman, K., Taylor, L.F., Mukherjee, P., Humphryes, N., Tsubouchi, H., and Macqueen, A.J. 2013. SUMO localizes to the central element of synaptonemal complex and is required for the full synapsis of meiotic chromosomes in budding yeast. *PLoS Genet.* **9**, e1003837.
Wang, S., Zickler, D., Kleckner, N., and Zhang, L. 2015. Meiotic crossover patterns: obligatory crossover, interference and homeostasis in a single process. *Cell Cycle* **14**, 305–314.
Watt, R. and Piper, P.W. 1997. *UBI4*, the polyubiquitin gene of *Saccharomyces cerevisiae*, is a heat shock gene that is also subject to catabolite derepression control. *Mol. Gen. Genet.* **253**, 439–447.
Wiborg, O., Pedersen, M.S., Wind, A., Berglund, L.E., Marcker, K.A., and Vuust, J. 1985. The human ubiquitin multigene family: some genes contain multiple directly repeated ubiquitin coding sequences. *EMBO J.* **4**, 755–759.
Yang, X., Song, M., Wang, Y., Tan, T., Tian, Z., Zhai, B., Yang, X., Tan, Y., Cao, Y., Dai, S., *et al.* 2022. The ubiquitin-proteasome system regulates meiotic chromosome organization. *Proc. Natl. Acad. Sci. USA* **119**, e2106902119.
Yoon, S.W., Lee, M.S., Xaver, M., Zhang, L., Hong, S.G., Kong, Y.J., Cho, H.R., Kleckner, N., and Kim, K.P. 2016. Meiotic prophase roles of Rec8 in crossover recombination and chromosome structure. *Nucleic Acids Res.* **44**, 9296–9314.
Zhang, L., Kim, K.P., Kleckner, N.E., and Storlazzi, A. 2011. Meiotic double-strand breaks occur once per pair of (sister) chromatids and, via Mec1/ATR and Tel1/ATM, once per quartet of chromatids. *Proc. Natl. Acad. Sci. USA* **13**, 20036–20041.
Zhang, L., Wang, S., Yin, S., Hong, S., Kim, K.P., and Kleckner, N. 2014. Topoisomerase II mediates meiotic crossover interference. *Nature* **511**, 551–556.
Zhu, Z., Bani Ismail, M., Shinohara, M., and Shinohara, A. 2020. SCF^{Cdc4} ubiquitin ligase regulates synaptonemal complex formation during meiosis. *Life Sci. Alliance* **8**, e202000933.
Zickler, D. and Kleckner, N. 1999. Meiotic chromosomes: integrating structure and function. *Annu. Rev. Genet.* **33**, 603–754.
Zickler, D. and Kleckner, N. 2015. Recombination, pairing, and synapsis of homologs during meiosis. *Cold Spring Harb. Perspect. Biol.* **7**, a016626.